

Electron-Transfer Acceleration Investigated by Time Resolved Infrared Spectroscopy

Published as part of the *Accounts of Chemical Research* special issue "Ultrafast Excited-State Processes in Inorganic Systems".

Antonín Vlček, Jr.,^{*,†,‡} Hana Kvapilová,[‡] Michael Towrie,[§] and Stanislav Zális[‡]

[†]School of Biological and Chemical Sciences, Queen Mary University of London, Mile End Road, London E1 4NS, United Kingdom

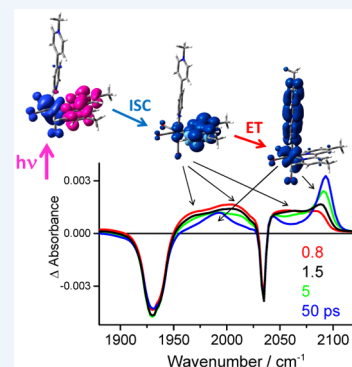
[‡]J. Heyrovský Institute of Physical Chemistry, Academy of Sciences of the Czech Republic, Dolejškova 3, CZ-182 23 Prague, Czech Republic

[§]Central Laser Facility, Research Complex at Harwell, STFC, Rutherford Appleton Laboratory, Harwell Oxford, Didcot, Oxfordshire OX11 0QX, United Kingdom

CONSPECTUS: Ultrafast electron transfer (ET) processes are important primary steps in natural and artificial photosynthesis, as well as in molecular electronic/photonic devices. In biological systems, ET often occurs surprisingly fast over long distances of several tens of angstroms. Laser-pulse irradiation is conveniently used to generate strongly oxidizing (or reducing) excited states whose reactions are then studied by time-resolved spectroscopic techniques. While photoluminescence decay and UV–vis absorption supply precise kinetics data, time-resolved infrared absorption (TRIR) and Raman-based spectroscopies have the advantage of providing additional structural information and monitoring vibrational energy flows and dissipation, as well as medium relaxation, that accompany ultrafast ET. We will discuss three cases of photoinduced ET involving the $\text{Re}^{\text{I}}(\text{CO})_3(\text{N},\text{N})$ moiety (N,N = polypyridine) that occur much faster than would be expected from ET theories.

$[\text{Re}(4\text{-}N\text{-methylpyridinium-pyridine})(\text{CO})_3(\text{N},\text{N})]^{2+}$ represents a case of excited-state picosecond ET between two different ligands that remains ultrafast even in slow-relaxing solvents, beating the adiabatic limit. This is caused by vibrational/solvational excitation of the precursor state and participation of high-frequency quantum modes in barrier crossing. The case of Re–tryptophan assemblies demonstrates that excited-state $\text{Trp} \rightarrow {}^*\text{Re}^{\text{II}}$ ET is accelerated from nanoseconds to picoseconds when the $\text{Re}^{\text{I}}(\text{CO})_3(\text{N},\text{N})$ chromophore is appended to a protein, close to a tryptophan residue. TRIR in combination with DFT calculations and structural studies reveals an interaction between the N,N ligand and the tryptophan indole. It results in partial electronic delocalization in the precursor excited state and likely contributes to the ultrafast ET rate. Long-lived vibrational/solvational excitation of the protein $\text{Re}^{\text{I}}(\text{CO})_3(\text{N},\text{N})\cdots\text{Trp}$ moiety, documented by dynamic IR band shifts, could be another accelerating factor. The last discussed process, back-ET in a porphyrin– $\text{Re}^{\text{I}}(\text{CO})_3(\text{N},\text{N})$ dyad, demonstrates that formation of a hot product accelerates highly exergonic ET in the Marcus inverted region.

Overall, it follows that ET can be accelerated by enhancing the electronic interaction and by vibrational excitation of the reacting system and its medium, stressing the importance of quantum nuclear dynamics in ET reactivity. These effects are experimentally accessible by time-resolved vibrational spectroscopies (IR, Raman) in combination with quantum chemical calculations. It is suggested that structural dynamics play different mechanistic roles in light-triggered ET involving electronically excited donors or acceptors than in ground-state processes. While TRIR spectroscopy is well suitable to elucidate ET processes on a molecular-level, transient 2D-IR techniques combining optical and two IR (or terahertz) laser pulses present future opportunities for investigating, driving, and controlling ET.



Electron transfer (ET) in molecular and biological systems occurs over time scales ranging from picoseconds to seconds and distances from units and tens of angstroms in small molecules and proteins to micrometers in extracellular appendages of “rock-breathing” bacteria.^{1–3} Depending on the distance and chemical nature of the medium bridging the donor and acceptor, ET mechanisms vary among electron tunneling, solvent-driven barrier crossing, hopping through redox intermediates, and a newly proposed^{1,4} flickering resonance. While ET through complex molecular media can be discussed

in terms of tunneling pathways, electron/hole superexchange, and tunneling timetables,³ recent research in ET theory emphasizes pathway interference and bridge dynamics.^{1,2,5,6} Biological systems have evolved in such a way that the rates of ET steps fit to the purpose: electrons are delivered to and from redox-enzyme

Received: November 7, 2014

Published: February 20, 2015

active sites with rates commensurate with those of substrate transformations, usually on a microsecond–millisecond time scale. On the other hand, ET is ultrafast (picosecond) when light energy or information needs to be captured. This is the case for photosynthesis reaction centers, cryptochromes, and DNA photolyase, where ultrafast photoinduced ET avoids side reactions of energetic photoexcited states, minimizes energy dissipation, and maintains the directionality and specificity of the ET process. Similarly, ultrafast photoinduced ET is desirable in artificial light-energy conversion, ideally producing long-lived charge-separated states. Molecular photonics and electronics also require ultrafast ET steps controlled by external stimuli.

ET rates often are sensitive to subtle variations of the bridge structure and surrounding medium. Some ET accelerating mechanisms are predicted by Marcus theory, such as diminishing outer reorganization energy by placing the reacting system in a nonpolar hydrophobic environment, increasing electronic delocalization within the donor and acceptor (to diminish inner reorganization energy), or increasing the donor–acceptor electronic coupling, H_{DA} . The latter provides a sensitive means of tuning rates of nonadiabatic ET that are proportional to $\langle H_{DA}^2 \rangle$, the mean square of the coupling element. This is the origin of the exponential decay of ET rates with the D–A distance, as well as of their dependence on the structure and chemical nature of the bridging medium.³ ET through complex molecular media (e.g., proteins) is mediated by a multitude of tunneling pathways, some of which could be dominating. Tuning the bridging medium to enhance coupling could accelerate ET considerably. For example, changing the attachment position of a Ru(bpy)₃ chromophore at a naphthalenebisimide (NBI) electron donor from the nitrogen atom to a naphthalene carbon atom accelerates photoinduced *Ru(bpy)₃ → NBI ET over 1000 times, from 63 ns to 52 ps.⁷ While about 20-fold acceleration is attributable to a driving-force increase, the rest is due to electronic coupling enhanced by a much larger NBI frontier orbital localization on the naphthyl core than on the nitrogens. Concerning proteins, a change of ET rate from ~200 μs to ~400 ps was accomplished by redesigning the Zn–myoglobin/cytochrome b₅ interface by a triple mutation at the myoglobin surface. The resulting tight complex has a high probability of attaining configurations with short distances between the cofactors, with the strongest-coupled ET pathways involving direct through-space tunneling between the hemes.^{8,9} Further opportunities for tuning ET kinetics emerge from bridge dynamics whereby fast ET can take place via strongly coupled pathways in off-equilibrium conformations attained by medium fluctuations. This is the case of proteins with multiple tunneling pathways but small average coupling element $\langle H_{DA} \rangle$. A case in point is Ru-modified cytochrome b₅₆₂, where such dynamic amplification increases the ET rate 140× at a constant Ru–Fe separation of 21 Å.^{6,10}

In this Account, we will discuss three cases of ultrafast ET involving Re^I(L)(CO)₃(N,N) chromophores (N,N = 2,2'-bipyridine (bpy)- or 1,10-phenanthroline (phen)-type ligands, L = N-coordinated ligand),¹¹ focusing on information provided by time-resolved IR spectroscopy (TRIR). Long excited-state lifetimes, redox activity, and photochemical and thermal stability, together with synthetic versatility, make these complexes widely used triggers of photochemical ET. Near-UV excitation prepares a Re → N,N metal to ligand charge transfer excited state (¹MLCT) that undergoes 80–150 fs intersystem crossing^{12,13} (ISC) to the lowest triplet ³MLCT, which is a strong oxidant as well as reductant. TRIR (and time-resolved resonance

Raman (TR³) or femtosecond stimulated Raman scattering (FSRS)) are important tools to study photoinduced ET, because they provide both kinetics and structural information. In the case of Re^I(L)(CO)₃(N,N), TRIR spectra in the region of C≡O stretching vibrations, $\nu(\text{CO})$, reflect changes in electronic and oxidation states, owing to their high sensitivity to Re → CO π back-donation.¹¹

The use of TRIR in photoinduced electron transfer is not limited to cases where the IR-active group (C≡O, C=O, N≡O, C≡N, C≡C, NCS, etc.) is part of the electron donor or acceptor. One of the first TRIR applications to photoinduced ET followed a Stark-effect shift of a C=O vibration of a spectator keto group upon oxidation of [3]-ferrocenophan-2-one by excited oxazine-1 dye. It was suggested that spectator-group vibrations will be sensitive to charge changes up to 6–7 Å away.¹⁴ Present TRIR technology allows monitoring reactions from a few hundreds of femtoseconds to milliseconds.^{15–17} On the ultrafast time scale, TRIR reports not only on structural changes but also on accompanying flows of vibrational energy and reorganization of the molecular environment (solvent, protein, or supramolecular media), which are manifested by dynamic spectral shifts and band narrowing.^{18,19}

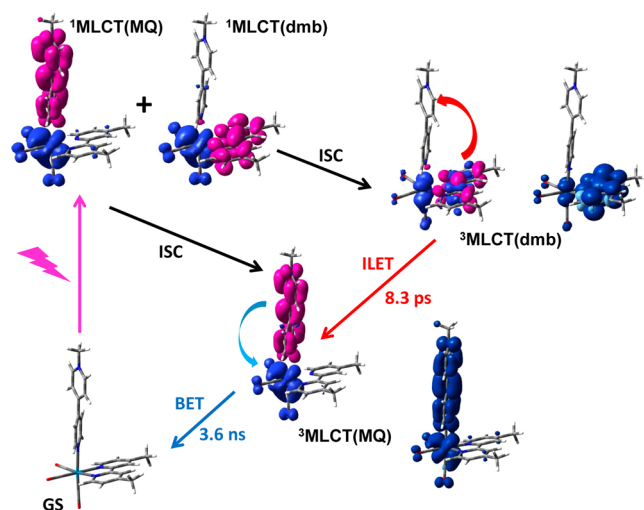
The following case studies document the utility of Re complexes as (ultra)fast triggers of photoinduced ET and reveal factors responsible for accelerating ET beyond rates estimated by conventional theories. It is shown that comprehensive mechanistic understanding often emerges from combining TRIR (and TR³) with other time-resolved spectroscopies and quantum-chemical calculations that provide²⁰ further information on structures, energies, and electron-density distributions of electronic and redox states, as well as on electronic coupling.

■ INTERLIGAND ELECTRON TRANSFER

Interligand ET (ILET) is a well-known problem of [Ru(bpy)₃]²⁺ photophysics where it amounts to electron localization dynamics after excitation and electron hopping between individual bpy ligands. Experimental studies^{21,22} and QM/MM calculations^{23,24} generally agree on subpicosecond scrambling of the excited electron followed by random charge transfer among the ligands. QM/MM also indicates ligand pairing, whereby the excited electron density is frequently localized on two ligands. ILET is driven by differential solvation of the bpy ligands and fluctuations of the solvent and intramolecular torsional modes.

We have investigated a different type of ILET (Scheme 1) that occurs energetically downhill by 0.3–0.5 eV between two nonequivalent ligands in [Re^I(MQ⁺)(CO)₃(dmb)]²⁺ (dmb = 4,4'-dimethyl-2,2'-bipyridine, MQ⁺ = N-methyl-4,4'-bipyridinium).^{25,26} Near-UV irradiation populates a Re → dmb ¹MLCT(dmb) excited state followed by 100–150 fs^{12,13} ISC to ³MLCT(dmb) that can be described as *[Re^{II}(MQ⁺)(CO)₃(dmb^{•-})]²⁺. ³MLCT(dmb) undergoes a dmb^{•-} → MQ⁺ ILET producing a ³MLCT(MQ) state *[Re^{II}(MQ⁺)(CO)₃(dmb)]²⁺. ILET is accompanied by planarization of the MQ ligand, from 35.9° to 0.2° (DFT-calculated). The photocycle is completed by a MQ⁺ → Re^{II} back electron transfer (BET) that regenerates the ground state.²⁷ DFT calculations show the excited electron density in both states to be strongly localized at the respective ligands (Scheme 1). Hence, ILET in [Re^I(MQ⁺)(CO)₃(dmb)]²⁺ can be discussed in terms of ET theories, rather than excited-state electron-density redistribution.

The ILET mechanism and kinetics were determined²⁶ by picosecond time-resolved absorption that showed decreasing

Scheme 1. Photoinduced ILET in $[\text{Re}^{\text{I}}(\text{MQ}^+)(\text{CO})_3(\text{dmb})]^{2+}$ and Accompanying Electron- And Spin-Density Changes^a


^aExcited states are characterized by electron-density reorganization relative to the ground state (blue, depletion; magenta, increase). In addition, $^3\text{MLCT}(\text{dmb})$ and $^3\text{MLCT}(\text{MQ})$ are characterized by unrestricted Kohn–Sham (UKS) spin-density distributions at TDDFT-optimized geometries, shown to the right of the reaction scheme. Irradiation excites both $^1\text{MLCT}(\text{MQ})$ and $^1\text{MLCT}(\text{dmb})$ transitions, which have comparable energies and oscillator strengths. Both singlets undergo ultrafast (fs) ISC to the corresponding triplets. ILET accounts for $\sim 40\%$ formation of $^3\text{MLCT}(\text{MQ})$; the rest is produced by direct ISC. The alternating blue and magenta regions at the dmb ligand of $^3\text{MLCT}(\text{dmb})$ indicate²⁰ an admixture of intraligand $\pi\pi^*$ character. Calculation: DFT, B3LYP, PCM-MeCN.

$\text{dmb}^{\bullet-}$ absorption at wavelengths shorter than 480 nm and a growing band at 630 nm attributable to MQ^{\bullet} . TR³ spectra (measured with a picosecond Kerr gate to remove emission) showed growing MQ^{\bullet} bands, some of which were strongly shifted from their ground-state positions. TRIR spectra in the $\nu(\text{CO})$ region (Figure 1) exhibit decaying and growing bands due to $^3\text{MLCT}(\text{dmb})$ and $^3\text{MLCT}(\text{MQ})$ states, respectively. In MeCN, the $\text{dmb}^{\bullet-} \rightarrow \text{MQ}^+$ ILET occurs with an 8.3 ps lifetime, much slower than the 0.26 ps average solvation response time,²⁸ indicating a predominantly nonadiabatic process. Making qualified assumptions about λ , the coupling term H_{DA} was estimated (eqs 1–3) as 130 cm^{-1} , providing an opportunity to control the rate by varying the solvent response times and indicating the possibility of transition to the adiabatic regime on going to slow-responding solvents. ILET dynamics were investigated in 22 solvents.²⁶ Surprisingly, the ILET lifetime varies over a very narrow range, between 8.3 ps (MeCN) and 17.5 ps (1,2-dimethoxyethane), independent of the solvent response time τ_{v} , the dielectric parameter $(1/\epsilon_{\text{op}} - 1/\epsilon_{\text{s}})$, thermal conductivity, viscosity (despite pyridinium-ring rotation during ILET), ionization potential, and through-solvent electronic coupling. Driving force ($-\Delta G^{\circ}$) variations seem to be the main factor affecting ILET kinetics. ILET remains fast even in slow-responding solvents: by eqs 1–3, lifetimes of ~ 90 ps were estimated²⁶ for PhCN, formamide, *N*-methyl-formamide, and MeOH ($\tau_{\text{v}} \approx 5$ ps), contrary to the experimental values of 8.5–11.8 ps. In ethylene glycol ($\tau_{\text{v}} \approx 15.3$ ps), a ~ 280 ps adiabatic ILET is predicted, whereas the experimental ILET time (14.0 ps) is 20-times shorter.

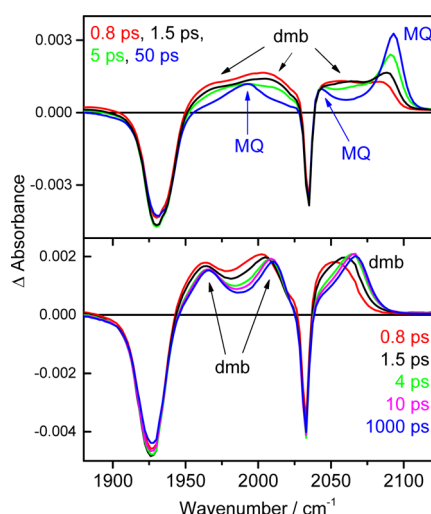


Figure 1. TRIR spectra of $[\text{Re}(\text{MQ}^+)(\text{CO})_3(\text{dmb})]^{2+}$ (top) and $[\text{Re}(\text{Etpy})(\text{CO})_3(\text{dmb})]^+$ (bottom) in MeCN at selected time delays after 400 nm, 50 fs excitation (ULTRA instrument¹⁷). Negative bands are due to ground-state depletion, positive features correspond to photogenerated transients. MQ and dmb denote bands due to $^3\text{MLCT}(\text{MQ})$ and $^3\text{MLCT}(\text{dmb})$, respectively. $[\text{Re}(\text{Etpy})(\text{CO})_3(\text{dmb})]^+$ does not undergo any photoreaction and its TRIR spectrum is characteristic^{11,29} of $^3\text{MLCT}(\text{dmb})$. The dynamic shift to higher wavenumbers (1.3 ps (74%); 11.6 ps (26%)) is attributable to vibrational and solvational relaxation.¹⁸ $[\text{Re}(\text{MQ}^+)(\text{CO})_3(\text{dmb})]^{2+}$ shows at early times the same $^3\text{MLCT}(\text{dmb})$ bands, which rapidly decay and simultaneously shift, as is apparent between 2050 and 2070 cm^{-1} . The $^3\text{MLCT}(\text{MQ})$ bands grow while the highest one shifts from ~ 2083 (at 0.8 ps) to 2093 cm^{-1} (≥ 50 ps).

$$k_{\text{NA}} = \frac{2\pi\langle H_{\text{DA}}^2 \rangle}{\hbar(4\pi\lambda k_{\text{B}}T)^{1/2}} \exp\left[-\frac{(\Delta G^{\circ} + \lambda)^2}{4\lambda k_{\text{B}}T}\right] \quad (1)$$

$$k_{\text{et}} = \frac{k_{\text{NA}}}{1 + H_{\text{A}}} \quad (2)$$

$$H_{\text{A}} = \frac{4\pi\langle H_{\text{DA}}^2 \rangle \tau_{\text{S}}}{\hbar\lambda} \quad (3)$$

Time resolved vibrational spectroscopies indicate possible reasons for ILET acceleration in slow-relaxing solvents. TR³ spectra show that certain MQ-localized vibrations change frequency on going from the ground state to $^3\text{MLCT}(\text{MQ})$.²⁶ The largest effect ($+53 \text{ cm}^{-1}$) was observed for the 1299 cm^{-1} band due to an MQ inter-ring C–C stretching vibration coupled with C–H bending, demonstrating the emergence of the MQ^{\bullet} quinoidal structure with a C=C bond between the two rings in $^3\text{MLCT}(\text{MQ})$. TRIR spectra at early times show decaying $^3\text{MLCT}(\text{dmb})$ $\nu(\text{CO})$ features and growing $^3\text{MLCT}(\text{MQ})$ bands that occur at higher wavenumbers (Figure 1). This behavior indicates the presence of high-frequency vibrations that are coupled to ILET and may contribute to its dynamics. TRIR also demonstrates that ILET occurs from an unequilibrated (“hot”) state to an unequilibrated product: $^3\text{MLCT}(\text{dmb})$ IR bands of a redox-inactive analogue $[\text{Re}(\text{Etpy})(\text{CO})_3(\text{dmb})]^+$ undergo a relaxation-induced dynamic upshift and narrowing on the same time scale as ILET in the MQ^+ complex.^{18,26} The highest $^3\text{MLCT}(\text{dmb})$ band of $[\text{Re}^{\text{I}}(\text{MQ}^+)(\text{CO})_3(\text{dmb})]^{2+}$ undergoes a similar dynamic shift while decaying (Figure 1). It follows that ILET occurs from a hot $^3\text{MLCT}(\text{dmb})$ state, simultaneously with its relaxation.

Moreover, the highest TRIR band of the $^3\text{MLCT}(\text{MQ})$ product in MeCN keeps shifting to higher wavenumbers until 30–40 ps after excitation, suggesting that it is formed hot - in a distorted geometry or solvent shell. MQ^* Raman bands also gradually shift higher and narrow with a 10–20 ps lifetime. Clearly, even the fast-responding MeCN solvent does not keep up with the electron-density redistribution, and ILET is accompanied by continuing relaxation.

In summary, ILET in $[\text{Re}(\text{MQ}^+)(\text{CO})_3(\text{dmb})]^{2+}$ is accelerated beyond the solvent-driven adiabatic rate by participation of intramolecular vibrations in barrier crossing and by vibrational/solvational excitation of the $^3\text{MLCT}(\text{dmb})$ precursor state. Accelerating vibrations need not only be the high-frequency $\nu(\text{CC})$ and $\nu(\text{CO})$ stretches observed by TR^3 and TRIR but also low-frequency high-amplitude modes that are anharmonically coupled to the high-frequency ones, together with vibrations of the first solvation shell. ET becomes independent of solvation dynamics, provided that the motion along the vibrational coordinate is faster than solvent rearrangement. This type of ET acceleration is treated by the Sumi–Marcus theory.³⁰ Vibrational/solvational excitation of the precursor state accelerates ILET by decreasing the reaction barrier (increasing $-\Delta G^\circ$) and by increasing the number of configurations for barrier crossing. (Configurational heterogeneity is manifested by large TRIR and TR^3 bandwidths at early times and narrowing in the course of relaxation.) ET acceleration due to involvement of intramolecular modes and precursor-state vibrational/solvational excitation is a more general mechanism. A case in point is a rigid π -stacked Zn-porphyrin–spacer–quinone assembly, where a subpicosecond ET becomes more prominent and faster at low temperatures, when solvent and vibrational relaxations slow down.³¹ Formation of a hot $^3\text{MLCT}(\text{MQ})$ indicates that the product intramolecular and solvational restructuring upon ILET is slower than the ET proper or that higher-energy nonequilibrated $^3\text{MLCT}(\text{dmb})$ configurations react along specific channels, retaining some extra energy. Present conclusions about ILET are extendable to interligand electron hopping in Ru(II) and Os(II) polypyridine photosensitizers that seems to occur with comparable rates and H_{DA} values.^{21,22,32,33}

■ TRYPTOPHAN OXIDATION BY EXCITED RHENIUM CHROMOPHORES

The $[\text{Re}(\text{MQ}^+)(\text{CO})_3(\text{dmb})]^{2+}$ case discussed above manifests the rare situation of a $\text{Re}(\text{CO})_3(\text{diimine})$ chromophore behaving as a photoreductant toward the axial ligand. Photo-induced oxidation of a ligand L upon MLCT excitation of $[\text{Re}(\text{L})(\text{CO})_3(\text{NN})]^{2+}$ is much more common.¹¹ It is used, for example, to trigger long-range electron transfer in biomolecules and oxidize their redox sites by near-UV irradiation: tryptophan and Cu^{I} in azurins (blue copper proteins),^{34–36} tyrosine in ribonucleotide reductase,³⁷ or guanine in DNA,^{38,39} helping us to understand biological electron transfer.

Tryptophan photooxidation was investigated in small-molecule complexes with tryptophan appended to the axial pyridine ligand, such as $[\text{Re}(4\text{-Trp-py})(\text{CO})_3(\text{bpy})]^+$ (Figure 2).⁴⁰ Whereas its picosecond TRIR spectra exhibit only $^3\text{MLCT}$ features undergoing relaxation-induced shifts within the first 30 ps, nanosecond TRIR (Figure 3) provides clear evidence for excited-state ET: a ~ 30 ns decay of the $^3\text{MLCT}$ bands accompanied by rise of two new bands at wavenumbers lower than in the ground state. This down-shift points to a higher electron density on $\text{Re}(\text{CO})_3$ and allows assigning the growing

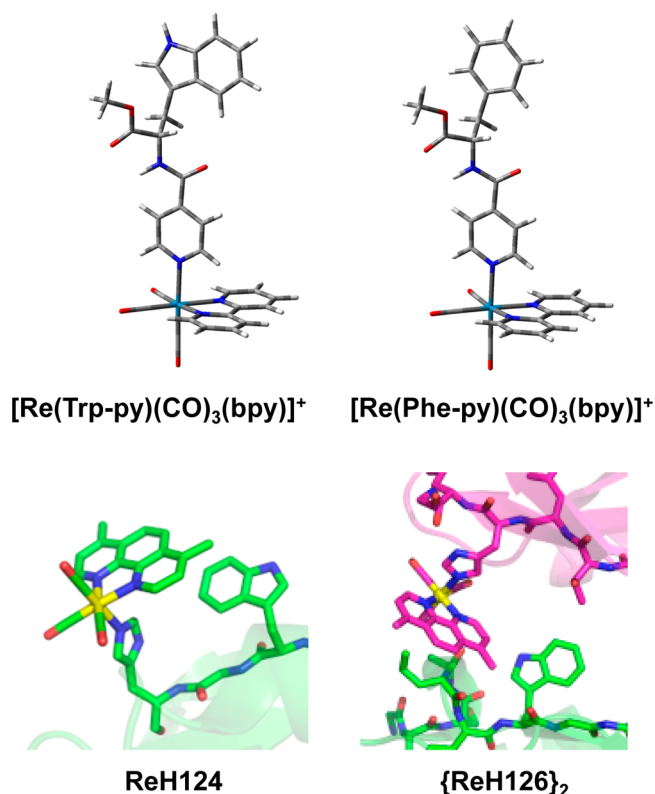


Figure 2. Re–tryptophan Re–phenylalanine assemblies. (top, left) $[\text{Re}(4\text{-Trp-py})(\text{CO})_3(\text{bpy})]^+$ and (top, right) $[\text{Re}(4\text{-Phe-py})(\text{CO})_3(\text{bpy})]^+$. Structures of phen and dmp analogues are virtually identical. (DFT-optimized: PBE0, PCM-MeCN). (bottom, left) Intramolecular $\text{Re}\cdots$ tryptophan moiety in $\text{ReH124} = \text{Re}(\text{CO})_3(\text{dmp})(\text{His124})(\text{Trp122})\text{Az}$ (PDB 2I7O).³⁴ (bottom, right) Intermolecular $\text{Re}\cdots$ tryptophan moiety in $\{\text{ReH126}\}_2 = \{\text{Re}(\text{CO})_3(\text{dmp})(\text{His126})(\text{Trp122})\text{Az}\}_2$ (PDB 4K9J).³⁶

features to a charge-separated state (CS): $[\text{Re}^{\text{I}}(\text{Trp}^{\bullet+}\text{-py})(\text{CO})_3(\text{bpy}^{\bullet-})]^+$. It follows that Re^{II} in the $^3\text{MLCT}$ state is reduced by a tryptophan $\rightarrow {}^*\text{Re}^{\text{II}}$ ET (Scheme 2). The CS then decays to the ground state by $\text{bpy}^{\bullet-} \rightarrow \text{Trp}^{\bullet+}$ BET. The forward and back ET occur with similar time constants of 30–40 ns. This behavior and kinetics are characteristic of a whole series of Re–tryptophan complexes. On the other hand, complexes with tyrosine or a redox-inactive phenylalanine instead of tryptophan exhibit only $^3\text{MLCT}$ TRIR features that decay much more slowly (~ 300 ns), with no evidence for ET (Figure 3).

$\text{Trp} \rightarrow {}^*\text{Re}^{\text{II}}$ ET becomes faster in a protein environment, when $\text{Re}^{\text{I}}(\text{CO})_3(\text{dmp})^+$ ($\text{dmp} = 4,7\text{-dimethyl-1,10-phenanthroline}$) is appended to a surface histidine close to a tryptophan residue. This is the case of Cu^{II} –azurins (Az) ReH124 and $\{\text{ReH126}\}_2$ (Figure 2, bottom). Their picosecond TRIR spectra (Figure 3, right) reveal conversion of $^3\text{MLCT}$ (${}^*\text{Re}^{\text{II}}(\text{CO})_3(\text{dmp}^{\bullet-})\cdots\text{Trp}$) to ^3CS ($\text{Re}^{\text{I}}(\text{CO})_3(\text{dmp}^{\bullet-})\cdots\text{Trp}^{\bullet+}$) with picosecond kinetics: <1 , 4–5, and 100–270 ps and 4–8 ns (ReH124)³⁵ and <1 and ~ 200 ps and 8 ns ($\{\text{ReH126}\}_2$),³⁶ eventually establishing an equilibrium. The structures indicate that the ET mechanism is different from the small-molecule complexes. The tryptophan indole in $[\text{Re}(\text{Trp-py})(\text{CO})_3(\text{N,N})]^+$ is ~ 12 Å apart from Re and points away from both Re and N,N. No indole–N,N interaction was detected by ^1H NMR (NOESY).⁴⁰ The ET occurs either through the pyridine ligand or through solvent. On the other hand, both proteins exhibit a Re–indole distance of ~ 8 Å and close $\text{dmp}\cdots$ indole contacts: nearly parallel (20.9° , 3.8 Å)

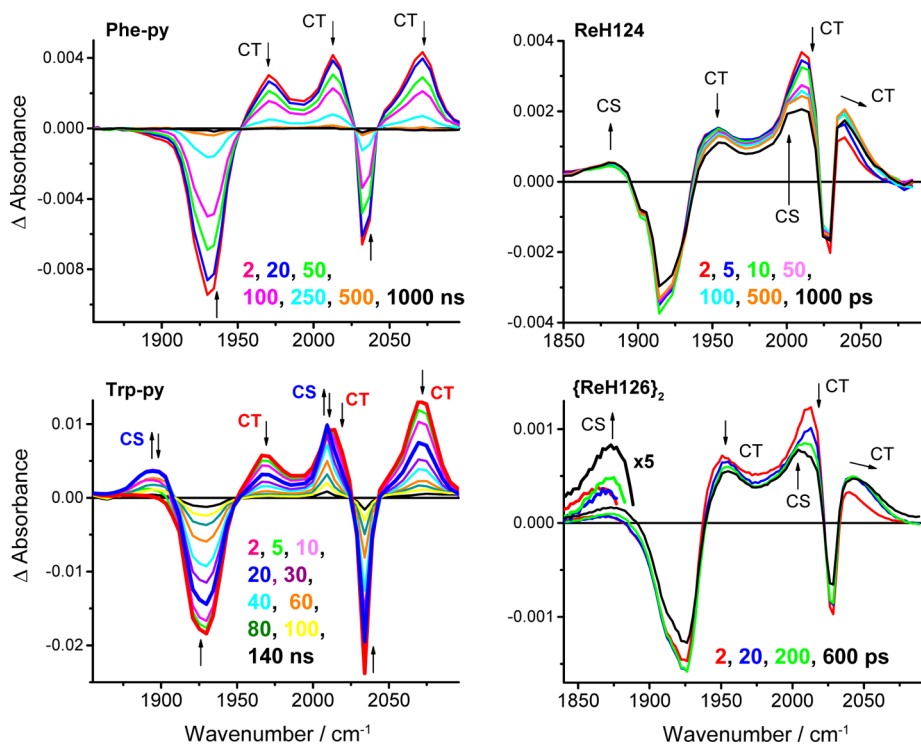
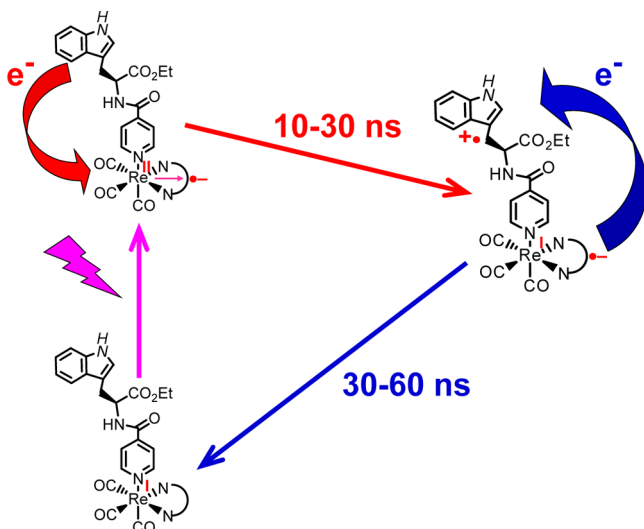


Figure 3. TRIR spectra of Re–tryptophan and Re–phenylalanine assemblies. (left, top) $[\text{Re}(4\text{-Phe-py})(\text{CO})_3(\text{bpy})]^+$ and (left, bottom) $[\text{Re}(4\text{-Trp-py})(\text{CO})_3(\text{bpy})]^+$ in MeCN after 355 nm, 0.8 ns excitation.⁴⁰ The highlighted 2 ns spectrum (red) shows only the three $^3\text{MLCT}$ features. The highlighted 20 ns spectrum (blue) shows two well-developed CS bands, plus residual $^3\text{MLCT}$. (right, top) ReH124 after 400 nm, 150 fs excitation.^{34,35} (right, bottom) $\{\text{ReH126}\}_2$ after 355 nm, 50 fs excitation.³⁶ Proteins in 50 mM $\text{KPi}/\text{D}_2\text{O}$ ($\text{pD} \approx 7.1$). (PIRATE,^{15,16} ULTRA¹⁷ for $\{\text{ReH126}\}_2$).

Scheme 2. Photoinduced ET in $[\text{Re}(\text{Trp-py})(\text{CO})_3(\text{N,N})]^+$ and Analogues^{40a}



^aThe time-constant ranges summarize values obtained for N,N = bpy, phen; 4-Trp-pyridine, 3-Trp-pyridine, or 4-Trp-imidazole in MeCN, DMF, DCM, or THF. No evidence was observed for $\text{Trp}^{+\bullet}$ deprotonation, which is expected to be much slower (≥ 130 ns)⁴¹ than BET.

in ReHis124 and intermolecular T-type with a 3.5 Å closest distance in $\{\text{ReH126}\}_2$. These $\text{dmp} \cdots \text{indole}$ interactions enable the ultrafast ET that occurs through a $\text{dmp}^{\bullet-}$ “bridge”: $^*\text{Re}^{\text{II}}(\text{CO})_3(\text{dmp}^{\bullet-}) \cdots \text{Trp} \rightarrow \text{Re}^{\text{I}}(\text{CO})_3(\text{dmp}^{\bullet-}) \cdots \text{Trp}^{\bullet+}$.³⁵ A $\text{dmp}-\text{CH}_3 \cdots \text{indole}$ interaction could participate in the

$\{\text{ReH126}\}_2$ ET pathway. (Tunneling through a methyl group was also suggested for ET from a photoexcited flavin anion to a DNA pyrimidine dimer.⁴²)

DFT calculations (Figure 4) indicate a partial delocalization between $\text{Re}(\text{CO})_3(\text{dmp})$ and indole in the $^3\text{MLCT}$ state of

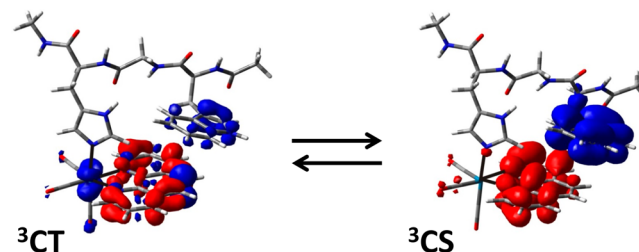


Figure 4. Electron-density differences of excited states of the $\text{Re}(\text{CO})_3(\text{phen})(\text{His124})(\text{Gly123})(\text{Trp122})$ moiety relative to the ground state.³⁵ Red, increase; blue, decrease. Alternating red and blue regions on phen in ^3CT indicate²⁰ a $\pi\pi^*$ intraligand contribution (UKS-DFT, PBE0, M06, CPCM- H_2O).

ReH124 before the ET proper, supporting the crucial role of the $\pi\pi$ interaction in mediating ET: whereas the excited electron density resides on dmp, the “hole” is delocalized between Re and the indole. This is in agreement with the very small ($+10$ cm^{-1}) shift of the highest $^3\text{MLCT}$ $\nu(\text{CO})$ IR band of both Re–azurins relative to the ground state, which contrasts with the small-molecule complexes, as well as a Re–azurin without a proximal tryptophan, showing a broad CT band shifted by $+25$ cm^{-1} (compare ReH124 and ReH124K122 (K = lysine) in Figure 5).³⁵ The small shift indicates that $\text{Re}(\text{CO})_3$ depopulation in ReH124 and $\{\text{ReH126}\}_2$ is smaller

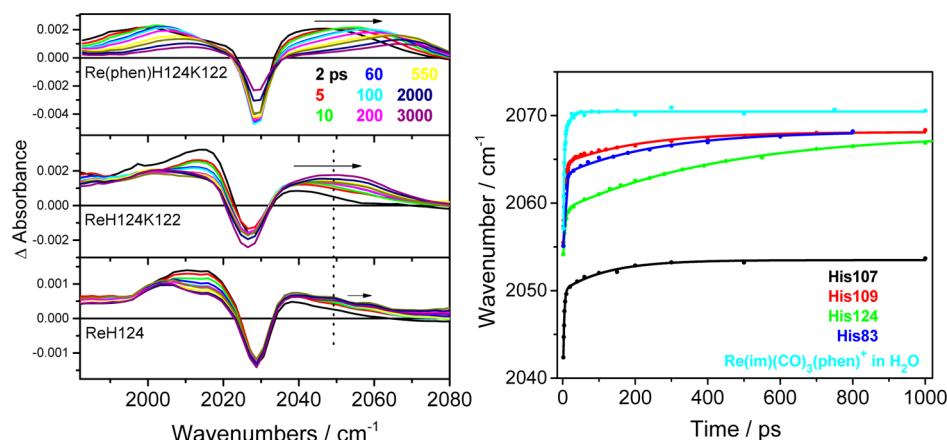


Figure 5. (left) TRIR dynamics of $\text{Re}(\text{CO})_3(\text{phen})(\text{His124})(\text{Lys122})\text{Az}$, $\text{ReHis124}(\text{Lys122})\text{Az}$, and ReHis124 in 50 mM $\text{KP}_1/\text{D}_2\text{O}$ ($\text{pD} \approx 7.1$) after 400 nm, 150 fs excitation.^{19,35} (right) time dependence of the wavenumber of the highest excited-state IR band of azurins labeled with $\text{Re}(\text{CO})_3(\text{phen})^+$ at His109, His124, His83, and $\text{Re}(\text{CO})_3(\text{dmp})^+$ at His107¹⁹ (PIRATE^{15,16}).

than would correspond to a $\text{Re} \rightarrow \text{dmb}^3\text{MLCT}$ transition. In the CS state, the tryptophan indole is fully oxidized, the extra electron density resides on dmp, and the Re^{I} oxidation state is restored (Figure 4). DFT together with TRIR thus suggest that the azurin $\{\text{Re}^{\text{I}}(\text{CO})_3(\text{dmp}) \cdots \text{Trp}\}$ moiety behaves as a single photoactive unit with $(\text{Re}, \text{indole}) \rightarrow \text{dmp}^3\text{CT}$ and $\text{indole} \rightarrow \text{dmp}^3\text{CS}$ excited states.³⁵

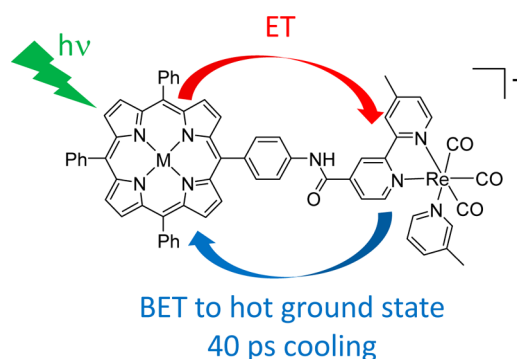
Vibrational/solvational excitation of the $^3\text{MLCT}$ precursor state could be another factor accelerating the $\text{Trp} \rightarrow \text{Re}^{\text{II}}$ ET in Re -azurins, similar to the MQ case. Figure 5 shows that relaxation-induced dynamic shifts of the highest CT band are much slower (≤ 1 ns) in proteins than small $[\text{Re}(\text{L})(\text{CO})_3(\text{N},\text{N})]^+$ complexes in solution, and dependent on the local structure (position) of the Re protein binding site.¹⁹ For ReH124 , the relaxation shift abates in 700–800 ps,³⁵ while it extends to nanoseconds for $\{\text{ReH126}\}_2$.³⁶ Relaxation is likely to include vibrational cooling together with restructuring of the solvated Re -azurin binding site in response to electron-density redistribution upon excitation.¹⁹

In summary, comparison of photoinduced ET in small-molecule complexes $[\text{Re}(\text{Trp-py})(\text{CO})_3(\text{N},\text{N})]^+$ and in Re -azurins shows that placing a $\text{Re}(\text{CO})_3(\text{dmp}) \cdots$ tryptophan moiety in a protein environment opens up a through-space ET pathway between the tryptophan indole and the dmp ligand. Tryptophan $\rightarrow \text{Re}^{\text{II}}(\text{CO})_3(\text{dmp})$ ET is accelerated from nanoseconds to picoseconds and can be employed to drive very fast long-range electron transfer via a hopping mechanism.^{34–36} Stacking π interactions also accelerate photooxidation of guanine in DNA by covalently appended and intercalated $\text{Re}^{\text{I}}(\text{py})(\text{CO})_3(\text{dppz})^+$ ($\text{dppz} = \text{dipyrido}[3,2\text{-}a:2',3'\text{-}c]\text{phenazine}$).^{38,39} This process is hard to study by TRIR because it occurs from a dppz-localized $^3\pi\pi^*$ state of $\text{Re}^{\text{I}}(\text{py})(\text{CO})_3(\text{dppz})^+$ whose TRIR features overlap with those of the ^3CS state. On the other hand, oxidized guanine is clearly observable.

■ RHENIUM–PORPHYRIN ASSEMBLY: INVERTED ET PRODUCES HOT GROUND STATE

A different ET mechanism operates in $\text{Re}^{\text{I}}(3\text{-picoline})(\text{CO})_3(\text{bpy})$ -metalloporphyrin dyads, which were introduced by Perutz and co-workers^{43,44} as potentially photocatalytic systems. Unlike the previous cases, $\text{Re}(\text{CO})_3(\text{bpy})$ is not the photoactive unit. Instead, a Mg or Zn tetraphenylporphyrin (MTPP) chromophore is excited at 560 or 600 nm, and ET

Scheme 3. Photoinduced ET in the $[\text{Re}(3\text{-Picoline})(\text{CO})_3(\text{bpy-M}(\text{TPP}))]^+$ Dyad ($\text{M} = \text{Mg}$ or Zn)⁴⁵



occurs from the porphyrin $\pi\pi^*$ S_1 state to the $\text{Re}(\text{CO})_3(\text{bpy})$ moiety (Scheme 3). The mechanism was unraveled by time-resolved visible absorption and TRIR informing on MTPP and $\text{Re}(3\text{-picoline})(\text{CO})_3(\text{bpy})^+$, respectively.⁴⁵ Both forward and back ETs take place on the early picosecond time scale. Forward ET occurs in the Marcus normal region, $-\Delta G^\circ \approx 0.32$ eV, whereas BET is inverted: $-\Delta G^\circ \approx 1.68$ eV, $\lambda \leq 1$ eV. TRIR (Figure 6) shows two bands of the CS state

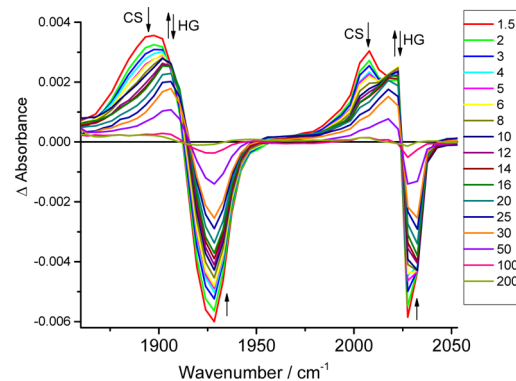


Figure 6. TRIR spectra of $[\text{Re}^{\text{I}}(3\text{-picoline})(\text{CO})_3(\text{bpy-MgTPP})]^+$ in PrCN after 600 nm, 150 fs excitation.⁴⁵ CS = $[\text{Re}^{\text{I}}(3\text{-picoline})(\text{CO})_3(\text{bpy}^{\bullet-}\text{-MgTPP}^{\bullet+})]^+$. HG = hot ground state. (PIRATE^{15,16})

$[\text{Re}^{\text{I}}(3\text{-picoline})(\text{CO})_3(\text{bpy}^{\bullet-}\text{-MgTPP}^{\bullet+})]^+$ shifted to lower wavenumbers from the ground state. The CS decay is faster

(20 ps) than the ground-state bleach recovery (35–40 ps). An intermediate state (HG) is involved, whose IR features are broad and shifted to lower wavenumbers relative to the ground state, but less than the CS bands. The HG features are attributable to a hot ground state, most likely excited in low-frequency modes that are anharmonically coupled to $\nu(\text{CO})$ vibrations.

The ET photocycle does not conform to conventional ET theories. Both ET steps are very fast, indicating large electronic coupling through the amide link. The ultrafast BET rate is surprising, given that it occurs deep in the inverted region and produces closed-shell products with no low-lying electronic states. Formation of a hot ground state indicates that BET occurs through parallel channels into higher vibrational states of the product. The effective driving force is lower by the amount corresponding to the product's extra vibrational energy, resulting in BET acceleration.⁴⁶ The actual observation of the hot ground state in the present system is unique, made possible by BET being faster than HG relaxation. From a practical point of view, ultrafast BET diminishes the yield and lifetime of the CS state that might be the desirable intermediate of light energy conversion or photocatalysis. It appears that the inverted effect alone need not be sufficient for prolonging lifetimes of CS states.

CONCLUDING REMARKS AND OUTLOOK

Vibrational/solvational excitation of the acceptor (or donor) in the precursor state accompanies ultrafast excited-state ET and can increase its rate above the adiabatic limit of solvent response (Figure 7, left). This is the case for ILET in

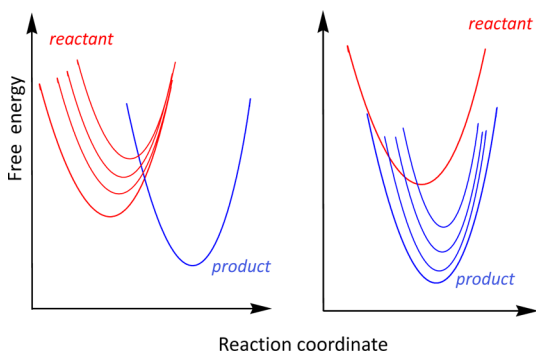


Figure 7. (left) In the Marcus normal region, precursor (red) vibrational/solvational excitation diminishes the barrier to the product (blue) and decreases the reorganization energy. (right) In the inverted region, formation of excited product occurs with a lower barrier and, possibly, higher reorganization energy caused by structural and solvational differences from the ground-state product.

$[\text{Re}(\text{MQ}^+)(\text{CO})_3(\text{dmb})]^{2+}$ and, possibly, also tryptophan photooxidation in azurins, where the excited Re chromophore remains “hot” for hundreds of picoseconds. Formation of hot charge-separated product becomes an important ET-accelerating mechanism in the inverted region (Figure 7, right), as is manifested by the Re–porphyrin dyad. Interestingly, the $[\text{Re}(\text{MQ}^+)(\text{CO})_3(\text{dmb})]^{2+}$ case also shows that vibrational/solvational excitation can persist through the ET leading to a hot product even if the driving force is relatively small.

Twinning the ET and structural/solvational dynamics suggests inherent differences between ET involving ground-state and electronically excited donors and acceptors. Ground-state ET (including flash-quench photogenerated oxidants or

reductants) involves Boltzmann-equilibrated reactants in a medium undergoing random thermal fluctuations. In contrast, optical excitation triggers not only the ET proper (by generating strong oxidants/reductants), but also vigorous relaxation movements whereby the reacting system dissipates energy and adjusts to the excitation-altered charge distribution. Excited-state ET occurs in a vibrationally excited fluctuating environment where intramolecular modes could contribute to barrier crossing, decrease the effective driving force, or transiently open up new strongly coupled pathways. This situation is not limited to ultrafast processes but applies also to slower ET from thermally equilibrated excited states. A recent study of IR spectral diffusion of $[\text{ReCl}(\text{CO})_3(\text{bpy})]$ in ground and equilibrated $^3\text{MLCT}$ states revealed lower solvent dielectric friction and longer-lived fluctuations in the vicinity of the excited complex.³⁷ In the context of biomolecular ET, it is important to consider structural dynamics of the whole system: the donor, acceptor, protein fold, and solvent. It would be desirable to monitor protein dynamics in the course of ET using IR reporters, possibly unnatural amino acids.

While the above examples demonstrate the ability of TRIR spectroscopy to elucidate electron transfer processes on a molecular level in systems ranging from small molecules to proteins, further opportunities are presented by modern two-dimensional IR techniques. For example, vibrational couplings and relative motions of donor, acceptor, and bridge groups could be followed by cross-peaks in transient 2D-IR spectra that employ one UV–vis and two IR pulses. Controlling ET emerges as a new research area: Quantum yield and rate of photoinduced ET in a dimethylaniline–guanosine–cytosine–anthracene and donor– $\text{C}\equiv\text{C}$ –Pt– $\text{C}\equiv\text{C}$ –acceptor dyads are diminished upon exciting bridge vibrations,^{48,49} whereas electron–hole separation at polymer heterojunctions is promoted by IR irradiation.⁵⁰ High-frequency IR excitation of specific vibrations could control ET by electron–phonon energy exchange in inelastic tunneling,² whereas terahertz pulses could open new ET pathways by extending the conformational space and facilitating fluctuations or changing environment dynamics.

AUTHOR INFORMATION

Corresponding Author

*E-mail: a.vlcek@qmul.ac.uk.

Funding

Financial support was provided by the Ministry of Education of the Czech Republic (LH13015), NIH, EPSRC, STFC and QMUL.

Notes

The authors declare no competing financial interest.

Biographies

Antonín Vlček studied chemistry at the Charles University (Prague) and received his Ph.D. from the Czechoslovak Academy of Sciences in 1984. Since 1996, he has been a professor of inorganic chemistry at Queen Mary, University of London, and an associated researcher at the J. Heyrovský Institute of Physical Chemistry (Prague). His work focuses on excited-state dynamics of transition metal complexes.

Hana Kvapilová studied chemistry at the Institute of Chemical Technology Prague and currently is a Ph.D. student at the J. Heyrovský Institute of Physical Chemistry (Prague). She investigates electron-transfer and photophysical phenomena in transition metal

complexes using quantum-chemical and time-resolved spectroscopic techniques.

Michael Towrie is Molecular and Structural Dynamics Group leader in the Central Laser Facility, Rutherford Appleton Laboratory. He has wide experience in advanced ultrafast vibrational spectroscopic techniques for fundamental molecular dynamics studies. For over 20 years his research has centered on development and scientific applications of lasers, detectors, and spectroscopic and imaging instrumentation including the Raman Kerr Gate and PIRATE, ULTRA, TR^MPS, and LIFEtime facilities.

Stanislav Zálíš studied chemistry at the University of Pardubice and received his Ph.D. from the Czechoslovak Academy of Sciences in 1977. Since then, he has worked at the J. Heyrovský Institute of Physical Chemistry (Prague), currently as a senior researcher. His expertise covers interpretation and prediction of physical properties of complex systems using quantum chemical methods.

ACKNOWLEDGMENTS

We thank Harry B. Gray and Robin N. Perutz for many exciting scientific discussions and a long-term collaboration on various aspects of electron transfer in Re–azurins and Re–porphyrin dyads, respectively.

REFERENCES

- Beratan, D. N.; Liu, C.; Migliore, A.; Polizzi, N. F.; Skourtis, S. S.; Zhang, P.; Zhang, Y. Charge Transfer in Dynamical Biosystems, or The Treachery of (Static) Images. *Acc. Chem. Res.* **2014**, DOI: 10.1021/ar500271d.
- Beratan, D. N.; Spiros, S.; Skourtis, S. S.; Balabin, I. A.; Balaeff, A.; Shahar Keinan, S.; Ravindra Venkatramani, R.; Dequan Xiao, D. Steering Electrons on Moving Pathways. *Acc. Chem. Res.* **2009**, *42*, 1669–1678.
- Gray, H. B.; Winkler, J. R. Long-Range Electron Transfer. *Proc. Natl. Acad. Sci. U.S.A.* **2005**, *102*, 3534–3539.
- Zhang, Y.; Liu, C.; Balaeff, A.; Skourtis, S. S.; Beratan, D. N. Biological Charge Transfer via Flickering Resonance. *Proc. Natl. Acad. Sci. U.S.A.* **2014**, *111*, 10049–10054.
- Balabin, I.; Onuchic, J. N. Dynamically Controlled Protein Tunneling Paths in Photosynthetic Reaction Centers. *Science* **2000**, *290*, 114–117.
- Prytkova, T. R.; Kurnikov, I. V.; Beratan, D. N. Coupling Coherence Distinguishes Structure Sensitivity in Protein Electron Transfer. *Science* **2007**, *315*, 622–625.
- Chaignon, F.; Falkenström, M.; Karlsson, S.; Blart, E.; Odobel, F.; Hammarström, L. Very Large Acceleration of the Photoinduced Electron Transfer in a Ru(bpy)₃–Naphthalene Bisimide Dyad Bridged on the Naphthyl Core. *Chem. Commun.* **2007**, 64–66.
- Xiong, P.; Nocek, J. M.; Vura-Weis, J.; Lockard, J. V.; Wasielewski, M. R.; Hoffman, B. M. Faster Interprotein Electron Transfer in a [Myoglobin, b5] Complex with a Redesigned Interface. *Science* **2010**, *330*, 1075–1078.
- Keinan, S.; Nocek, J. M.; Hoffman, B. M.; Beratan, D. N. Interfacial Hydration, Dynamics and Electron Transfer: Multi-scale ET Modeling of the Transient [Myoglobin, Cytochrome b5] complex. *Phys. Chem. Chem. Phys.* **2012**, *14*, 13881–13889.
- Gray, H. B.; Winkler, J. R. Electron Tunneling through Proteins. *Q. Rev. Biophys.* **2003**, *36*, 341–372.
- Vlček, A., Jr. Ultrafast Excited-State Processes in Re(I) Carbonyl-Diimine Complexes: From Excitation to Photochemistry. *Top. Organomet. Chem.* **2010**, *29*, 73–114.
- Cannizzo, A.; Blanco-Rodríguez, A. M.; Nahhas, A.; Šebera, J.; Zálíš, S.; Vlček, A., Jr.; Chergui, M. Femtosecond Fluorescence and Intersystem Crossing in Rhenium(I) Carbonyl-Bipyridine Complexes. *J. Am. Chem. Soc.* **2008**, *130*, 8967–8974.
- El Nahhas, A.; Consani, C.; Blanco-Rodríguez, A. M.; Lancaster, K. M.; Braem, O.; Cannizzo, A.; Towrie, M.; Clark, I. P.; Zálíš, S.; Chergui, M.; Vlček, A., Jr. Ultrafast Excited-State Dynamics of Rhenium(I) Photosensitizers [Re(Cl)(CO)₃(N,N)] and [Re-(imidazole)(CO)₃(N,N)]⁺: Diimine Effects. *Inorg. Chem.* **2011**, *50*, 2932–2943.
- Volk, M.; Gilch, P.; Kompa, C.; Haselsberger, R.; Härter, P.; Stöckl, M.; Scherer, W.; Latzel, K.; Michel-Beyerle, M.-E. Carbonyl Spectator Bonds as Sensitive Sensors for Charge Transfer Reactions on the Femtosecond Time Scale. *J. Phys. Chem. A* **2000**, *104*, 4984–4988.
- Towrie, M.; Grills, D. C.; Dyer, J.; Weinstein, J. A.; Matousek, P.; Barton, R.; Bailey, P. D.; Subramaniam, N.; Kwok, W. M.; Ma, C. S.; Phillips, D.; Parker, A. W.; George, M. W. Development of a Broadband Picosecond Infrared Spectrometer and its Incorporation into an Existing Ultrafast Time-Resolved Resonance Raman, UV/Visible, and Fluorescence Spectroscopic Apparatus. *Appl. Spectrosc.* **2003**, *57*, 367–380.
- Towrie, M.; Parker, A. W.; Vlček, A., Jr.; Gabrielsson, A.; Blanco Rodríguez, A. M. A High Sensitivity Femtosecond to Microsecond Time Resolved Infrared Vibrational Spectrometer. *Appl. Spectrosc.* **2005**, *59*, 467–473.
- Greetham, G.; Burgos, P.; Cao, Q.; Clark, I. P.; Codd, P.; Farrow, R.; George, M. W.; Kogimtzis, M.; Matousek, P.; Parker, A. W.; Pollard, M.; Robinson, D.; Xin, Z.-J.; Towrie, M. ULTRA - A Unique Instrument for Time-Resolved Spectroscopy. *Appl. Spectrosc.* **2010**, *64*, 1311–1319.
- Liard, D. J.; Busby, M.; Matousek, P.; Towrie, M.; Vlček, A., Jr. Picosecond Relaxation of ³MLCT Excited States of [Re(Etpy)-(CO)₃(dmb)]⁺ and [Re(Cl)(CO)₃(bpy)] as Revealed by Time-Resolved Resonance Raman, IR and UV–Vis Absorption Spectroscopy. *J. Phys. Chem. A* **2004**, *108*, 2363–2369.
- Blanco-Rodríguez, A. M.; Busby, M.; Ronayne, K. L.; Towrie, M.; Gráđinaru, C.; Sudhamsu, J.; Šýkora, J.; Hof, M.; Zálíš, S.; Di Bilio, A. J.; Crane, B. R.; Gray, H. B.; Vlček, A., Jr. Relaxation Dynamics of Pseudomonas aeruginosa Re^I(CO)₃(α -diimine)(HisX)⁺ (X = 83, 107, 109, 124, 126)Cu^{II} Azurins. *J. Am. Chem. Soc.* **2009**, *131*, 11788–11800.
- Vlček, A., Jr.; Zálíš, S. Modeling of Charge Transfer Transitions and Excited States in d6 Transition Metal Complexes by DFT Techniques. *Coord. Chem. Rev.* **2007**, *251*, 258–287.
- Wallin, S.; Davidsson, J.; Modin, J.; Hammarström, L. Femtosecond Transient Absorption Anisotropy Study on [Ru-(bpy)₃]₃²⁺ and [Ru(bpy)(py)₄]₂²⁺. *J. Phys. Chem. A* **2005**, *109*, 4697–4704.
- Yeh, A. T.; Shank, C. V.; McCusker, J. K. Ultrafast Electron Localization Dynamics Following Photo-Induced Charge Transfer. *Science* **2000**, *289*, 935–938.
- Moret, M.-E.; Tavernelli, I.; Chergui, M.; Rothlisberger, U. Electron Localization Dynamics in the Triplet Excited State of [Ru(bpy)₃]₃²⁺ in Aqueous Solution. *Chem.—Eur. J.* **2010**, *16*, 5889–5894.
- Hoff, D. A.; Silva, R.; Rego, L. G. C. Subpicosecond Dynamics of Metal-to-Ligand Charge-Transfer Excited States in Solvated [Ru(bpy)₃]₃²⁺ Complexes. *J. Phys. Chem. C* **2011**, *115*, 15617–15626.
- Westmoreland, T. D.; Le Bozec, H.; Murray, R. W.; Meyer, T. J. Multiple-State Emission and Intramolecular Electron Transfer Quenching in Rhenium(I) bpy Based Chromophore-Quencher Complexes. *J. Am. Chem. Soc.* **1983**, *105*, 5952–5954.
- Liard, D. J.; Busby, M.; Farrell, I. R.; Matousek, P.; Towrie, M.; Vlček, A., Jr. Mechanism and Dynamics of Interligand Electron Transfer in [ReMQ⁺](CO)₃(dmb)]²⁺. An Ultrafast Time-Resolved Visible and IR Absorption, Resonance Raman and Emission Study (dmb = 4,4'-dimethyl-2,2'-bipyridine, MQ⁺ = N-methyl-4,4'-bipyridinium). *J. Phys. Chem. A* **2004**, *108*, 556–567.
- Liard, D. J.; Kleverlaan, C. J.; Vlček, A., Jr. Solvent-Dependent Dynamics of the MQ⁺ → Re^{II} Excited-State Electron Transfer in [Re(MQ⁺)(CO)₃(dmb)]₃²⁺ (dmb = 4,4'-Dimethyl-2,2'-bipyridine,

MQ^+ = *N*-Methyl-4,4'-bipyridinium). *Inorg. Chem.* **2003**, *42*, 7995–8002.

(28) Horng, M. L.; Gardecki, J. A.; Papazyan, A.; Maroncelli, M. Subpicosecond Measurements of Polar Solvation Dynamics: Coumarin 153 Revisited. *J. Phys. Chem.* **1995**, *99*, 17311–17337.

(29) Dattelbaum, D. M.; Omberg, K. M.; Hay, P. J.; Gebhart, N. L.; Martin, R. L.; Schoonover, J. R.; Meyer, T. J. Defining Electronic Excited States Using Time-Resolved Infrared Spectroscopy and Density Functional Theory Calculations. *J. Phys. Chem. A* **2004**, *108*, 3527–3536.

(30) Sumi, H.; Marcus, R. A. Dynamical Effects in Electron Transfer Reactions. *J. Chem. Phys.* **1986**, *84*, 4894–4914.

(31) Kang, Y. K.; Duncan, T. V.; Therien, M. J. Temperature-Dependent Mechanistic Transition for Photoinduced Electron Transfer Modulated by Excited-State Vibrational Relaxation Dynamics. *J. Phys. Chem. B* **2007**, *111*, 6829–6838.

(32) Shaw, G. B.; Brown, C. L.; Papanikolas, J. M. Investigations of Interligand Electron Transfer in Polypyridyl Complexes of Os(II) Using Femtosecond Polarization Anisotropy Methods: Examination of $\text{Os}(\text{bpy})_3^{2+}$ and $\text{Os}(\text{bpy})_2(\text{mab})^{2+}$. *J. Phys. Chem. A* **2002**, *106*, 1483–1495.

(33) Waterland, M. R.; Kelley, D. F. Photophysics and Relaxation Dynamics of $\text{Ru}(4,4'\text{-Dicarboxy-2,2'}\text{-bipyridine})_2\text{cis}(\text{NCS})_2$ in Solution. *J. Phys. Chem. A* **2001**, *105*, 4019–4028.

(34) Shih, C.; Museth, A. K.; Abrahamsson, M.; Blanco-Rodríguez, A. M.; Di Bilio, A. J.; Sudhamsu, J.; Crane, B. R.; Ronayne, K. L.; Towrie, M.; Vlček, A., Jr.; Richards, J. H.; Winkler, J. R.; Gray, H. B. Tryptophan-Accelerated Electron Flow Through Proteins. *Science* **2008**, *320*, 1760–1762.

(35) Blanco-Rodríguez, A. M.; Di Bilio, A. J.; Shih, C.; Museth, A. K.; Clark, I. P.; Towrie, M.; Cannizzo, A.; Sudhamsu, J.; Crane, B. R.; Sýkora, J.; Winkler, J. R.; Gray, H. B.; Zálíš, S.; Vlček, A., Jr. Phototriggering Electron Flow through ReI-Modified *Pseudomonas aeruginosa* Azurins. *Chem.—Eur. J.* **2011**, *17*, 5350–5361.

(36) Takematsu, K.; Williamson, H.; Blanco-Rodríguez, A. M.; Sokolová, L.; Nikolovski, P.; Kaiser, J. T.; Towrie, M.; Clark, I. P.; Vlček, A., Jr.; Winkler, J. R.; Gray, H. B. Tryptophan-Accelerated Electron Flow Across a Protein–Protein Interface. *J. Am. Chem. Soc.* **2013**, *135*, 15515–15525.

(37) Reece, S. Y.; Seyedsayamdost, M. R.; Stubbe, J.; Nocera, D. G. Direct Observation of a Transient Tyrosine Radical Competent for Initiating Turnover in a Photochemical Ribonucleotide Reductase. *J. Am. Chem. Soc.* **2007**, *129*, 13828–13830.

(38) Olmon, E. D.; Sontz, P. A.; Blanco-Rodríguez, A. M.; Towrie, M.; Clark, I. P.; Vlček, A., Jr.; Barton, J. K. Charge Photoinjection in Intercalated and Covalently Bound $[\text{Re}(\text{CO})_3(\text{dppz})(\text{py})]^+$ - DNA Constructs Monitored by Time-Resolved Visible and Infrared Spectroscopy. *J. Am. Chem. Soc.* **2011**, *133*, 13718–13730.

(39) Cao, Q.; Creely, C. M.; Davies, E. S.; Dyer, J.; Easun, T. L.; Grills, D. C.; McGovern, D. A.; McMaster, J.; Pitchford, J.; Smith, J. A.; Sun, X.-Z.; Kelly, J. M.; George, M. W. Excited State Dependent Electron Transfer of a Rhenium-Dipyridophenazine Complex Intercalated between the Base Pairs of DNA: A Time-Resolved UV-Visible and IR Absorption Investigation into the Photophysics of fac- $[\text{Re}(\text{CO})_3(\text{F}_2\text{dppz})(\text{py})]^+$ Bound to either $[\text{poly}(\text{dA-dT})_2]$ or $[\text{poly}(\text{dG-dC})_2]$. *Photochem. Photobiol. Sci.* **2011**, *10*, 1355–1364.

(40) Blanco-Rodríguez, A. M.; Towrie, M.; Sýkora, J.; Zálíš, S.; Vlček, A., Jr. Photoinduced Intramolecular Tryptophan Oxidation and Excited-State Behavior of $[\text{Re}^{\text{I}}(\text{L-AA})(\text{CO})_3(\text{diimine})]^+$ (L = Pyridine or Imidazole, AA = Tryptophan, Tyrosine, Phenylalanine). *Inorg. Chem.* **2011**, *50*, 6122–6134.

(41) Sjödin, M.; Styring, S.; Wolpher, H.; Xu, Y.; Sun, L.; Hammarström, L. Switching the Redox Mechanism: Models for Proton-Coupled Electron Transfer from Tyrosine and Tryptophan. *J. Am. Chem. Soc.* **2005**, *127*, 3855–3863.

(42) Prytkova, T. R.; Beratan, D. N.; Skourtis, S. S. Photoselected Electron Transfer Pathways in DNA Photolyase. *Proc. Natl. Acad. Sci. U.S.A.* **2007**, *104*, 802–807.

(43) Gabrielsson, A.; Hartl, F.; Lindsay Smith, J. R.; Perutz, R. N. Photo-induced Ligand Substitution at a Remote Site via Electron Transfer in a Porphyrin-Appended Rhenium Carbonyl Supermolecule. *Chem. Commun.* **2002**, 950–951.

(44) Gabrielsson, A.; Lindsay Smith, J. R.; Perutz, R. N. Remote Site Photosubstitution in Metalloporphyrin–Rhenium Tricarbonylbipyridine Assemblies: Photo-reactions of Molecules with Very Short Lived Excited States. *Dalton Trans.* **2008**, 4259–4269.

(45) Gabrielsson, A.; Hartl, F.; Zhang, H.; Lindsay Smith, J. R.; Towrie, M.; Vlček, A., Jr.; Perutz, R. N. Ultrafast Charge Separation in a Photo-Reactive Rhenium-Appended Porphyrin Assembly Monitored by Picosecond Transient Infrared Spectroscopy. *J. Am. Chem. Soc.* **2006**, *128*, 4253–4266.

(46) Jortner, J.; Bixon, M. Intramolecular Vibrational Excitations Accompanying Solvent-Controlled Electron Transfer Reactions. *J. Chem. Phys.* **1988**, *88*, 167–170.

(47) Kiefer, L. M.; King, J. T.; Kubarych, K. J. Equilibrium Excited State Dynamics of a Photo-Activated Catalyst Measured with Ultrafast Transient 2DIR. *J. Phys. Chem. A* **2014**, *118*, 9853–9860.

(48) Lin, Z.; Lawrence, C. M.; Xiao, D.; Kireev, V. V.; Skourtis, S. S.; Sessler, J. L.; Beratan, D. N.; Rubtsov, I. V. Modulating Unimolecular Charge Transfer by Exciting Bridge Vibrations. *J. Am. Chem. Soc.* **2009**, *131*, 18060–18062.

(49) Delor, M.; Scattergood, P. A.; Sazanovich, I. V.; Parker, A. W.; Greetham, G. M.; Meijer, A. J. H. M.; Towrie, M.; Weinstein, J. A. Toward Control of Electron Transfer in Donor-Acceptor Molecules by Bond-Specific Infrared Excitation. *Science* **2014**, *346*, 1492–1495.

(50) Bakulin, A. A.; Rao, A.; Pavelyev, V. G.; van Loosdrecht, P. H. M.; Pshenichnikov, M. S.; Niedzialek, D.; Cornil, J.; Beljonne, D.; Friend, R. H. The Role of Driving Energy and Delocalized States for Charge Separation in Organic Semiconductors. *Science* **2012**, *335*, 1340–1344.